International Journal of Engineering Trends and Technology
ISSN: 2231-5381/ https://doi.org/10.14445/22315381/IJETT-V74I8P132

Volume 74 Issue 8, 483-495, August 2026

Original Article

Progression-Aware Synthetic Image Generation with Explainable Deep Learning Framework for Rare Skin Disease Detection and Classification

P Muthamil Selvan[1], S Pazhanirajan[2], K Abhirami[3]

[1,2]*Department of Computer Science and Engineering, Annamalai University, Tamil Nadu, India.*
[3]*Department of Computer Science and Engineering, Kings College of Engineering, Tamil Nadu, India.*

[1]*Corresponding Author : csemuthamilselvan@gmail.com*

Received: 25 February 2026 Revised: 27 July 2026 Accepted: 05 August 2026 Published: 29 August 2026

Abstract *- Rare diseases affect approximately 300 to 400 million individuals around the world, posing major difficulties in medical diagnosis. Among these, rare skin disorders represent a significant subset, frequently characterized by intricate visual patterns and higher inter-class similarity, which creates substantial obstacles in precise diagnosis. Artificial Intelligence (AI)-driven research for rare skin diseases has accelerated rapidly, unlocking new potential for timely, precise diagnosis and better long-term management strategies. DL techniques have considerably enhanced the classification and detection of skin diseases, including rare skin diseases, across clinical image analysis. However, the availability of adequate labeled datasets for rare skin diseases is limited, which restricts the generality of deep learning systems. To address these challenges, this study presents a Progression-Aware Synthetic Learning Framework for Rare Skin Disease Diagnosis (PASLF-RSDD). The primary objective of this study is to enhance rare skin disease diagnosis through multi-modal synthetic data augmentation, thereby improving the performance of the Deep Learning Model. Initially, the proposed PASLF-RSDD model employs Multi-Modal CycleGAN for synthetic image generation. Following that, high-level discriminative features are extracted using DenseNet121 integrated with Squeeze-and-Excitation blocks for improved feature representation. The extracted features are then passed into a bidirectional convolutional long-short term memory network for accurate rare skin condition classification, such as Elastosis Perforans Serpiginosa, Lentigo Maligna, Nevus Sebaceus, and Blue Naevus. The hyperparameters of the proposed BiConvLSTM classifier are automatically optimized by the Ant Lion Optimizer (ALO), which can effectively search the hyperparameter space to find optimal parameter combinations. This optimization approach stabilizes convergence, reduces the manual selection of parameters in the optimization, and improves the classification performance. Eigen-CAM is embedded to produce explanations in the form of images that make the model more interpretable and boost confidence in the diagnosis predictions by clinicians. The proposed PASLF-RSDD framework was evaluated experimentally with a benchmark dataset called DermaEvolve. Comparative analysis shows that they have better classification results in several evaluation metrics.*

Keywords *- Rare Skin Disease, Deep Learning, Multi-Modal CycleGAN, Feature extraction, Hyperparameter optimization, Explainable artificial intelligence.*

1. Introduction

Rare Diseases (RD) are categorized by a limited prevalence within the population. There is no clear consensus regarding the proportion of affected individuals with a disease to be regarded as an RD [1]. As yet, there are nearly 7000 RDs, and new RDs are recognized every week. Despite their low prevalence, these diseases might impact over 400 million individuals all over the world. RD is often inherited genetically, leading to chronic diseases that are initially in adulthood or later in life [2]. Several RDs are progressive, disabling, and severe, with restricted treatment possibilities, leaving patients with poor clinical outcomes if misdiagnosed or undiagnosed for a long time. A main difficulty in the RD management is the heterogeneity and complexity of indications [3]. These diseases frequently have overlapping medical expressions with a common disease, which makes diagnosis specifically complex for medical care providers. In addition, multiple tests lack well-performed, normalized tests or diagnostic standards, further complicating the procedure for diagnosis [4]. As an outcome, patients may be subjected to a comprehensive testing process and consultation with many experts prior to receiving a precise diagnosis. This delay may result in inadequate treatment or irreparable damage, highlighting the immediate demand for improved diagnostic tools [5]. In recent years, the medical care domain has experienced a significant transformation due to advanced

medical image processing techniques. Artificial intelligence (AI) models offer novel approaches to examining medical images, with unprecedented outcomes [6]. Actually, AI systems could acquire the expertise of several specialized experts, determine novel biomarkers by testing the existing data, and regulate the treatment and diseases detention process [7]. The effective implementation of an AI model is based on the leverage of huge datasets that denote the varied manifestations of the disease under consideration. Consequently, not all clinical parts are leveraging innovation in AI at the same speed [8].

Where several areas, such as oncology or radiology, are already leveraging these emerging technologies, their application in areas like this is still complex because of the lack of the needed widespread datasets. ML methods are low sensitive to data shortage and, therefore, they have been successfully implemented in many research studies with comparatively limited datasets [9]. Moreover, large-scale datasets are significant to train more advanced techniques like DL successfully. In this part, the DL method supports public health-related programs by systematic contact tracing, predictive modeling, and monitoring the spread of the virus for outbreak detection. In RD management, DL enhances precision medicine practices by employing high-data patient registries for identifying potential organizations, thus improving diagnosis, prevention, treatment, and monitoring according to people's genetic standards [10].

Deep learning has been found to greatly aid in automated diagnosis of skin diseases; the current studies are mostly dedicated to common dermatological disorders and demand large volumes of annotated data to train deep learning models successfully. In these cases, the limited number of clinically validated images of rare skin diseases significantly limits the learning capabilities and generalizability of traditional deep learning models. Data augmentation and transfer learning are recent methods proposed for mitigating data scarcity with limited success at retaining disease progression characteristics and lesion-specific visual patterns. Diagnostic frameworks also exist, which focus on synthetic image generation, feature extraction, hyperparameter optimization, and explainability, but not on their interlinkage. The absence of clinically meaningful predictions also limits the implementation of AI in dermatological diagnosis to a certain extent.

To address data scarcity in rare skin disease diagnosis, this paper introduces a Progression-Aware Synthetic Learning Framework for Rare Skin Disease Diagnosis (PASLF-RSDD). The PASLF-RSDD system aims to improve diagnostic performance through multi-modal synthetic data augmentation. The PASLF-RSDD approach follows a multi-stage pipeline comprising synthetic image generation, feature extraction, classification, hyperparameter optimization, and explainable artificial intelligence. The performance validation of the proposed PASLF-RSDD model is carried out using the benchmark dataset under several metrics. The main contributions of the work are as follows:

- Develop a multi-modal synthetic data generation approach using CycleGAN for generating realistic and progression-aware synthetic images, thereby reducing data scarcity issues in rare disease datasets.
- Design a DenseNet121 integrated with Squeeze-and-Excitation (SE) for feature extraction, allowing improved channel-wise feature recalibration and better representation of subtle pathological patterns in skin images.
- Present a bidirectional convolutional long-short term memory (BiConvLSTM) for rare skin disease classification, which efficiently learns spatial dependencies and sequential progression patterns among features.
- Use the Ant Lion Optimizer (ALO) for hyperparameter tuning, enhancing convergence stability and classification performance with reduced manual intervention.
- Incorporate Eigen-CAM for visual explainability, which highlights disease-relevant regions and improves the transparency and clinical interpretability of the proposed model.
- Conduct extensive simulations on the benchmark DermaEvolve dataset and demonstrate the improved performance of the model across multiple evaluation metrics.

2. Literature Review

Chen et al. [11] proposed RareAlert, a proactive screening system developed for common application at every primary medical encounter that predicts patient-level RD threads under routinely accessible at primary care data only by utilizing heterogeneous clinical reasoning through Large Language Models (LLMs). Tang [12] introduced a hybrid architecture incorporating MRI and CT procedures, integrating CNN and a Transformer framework and presenting mechanism for adversarial domain adaptation. The specialized CNN encoder captures detailed local attributes, and the transformer module acquires long-term inter-modal relationships. The gradient reversal domain discriminator modifies the feature-level distribution of various scanning gadgets to assure the technique’s device. Wang et al. [13] introduced the system of AI to detect the disease and manage RD.

Recent developments encompass few-shot learning models created to avoid data shortage, medically demonstrated foundation methods, which improves diagnostic reliability over organizations, and multi-modal AI architecture. Increasingly, AI is recognized for speeding up diagnoses and refining support networks for rare diseases. Napolitano et al. [14] presented the leverage of AI in drug development, with a robust concentration on the particular attainments and difficulties associated with RD. AI

can allow unavailable methods depending to the extensive incorporation of varied datasets. Significant barriers hinder the widespread adoption of AI within the cautious pharmaceutical sector, which is prone to quick disillusionment.

Wojtara et al. [15] analyzed current development in AI and how AI could be implemented to streamline RD disease detection and enhance the treatment. The utilization of AI could surpass certain traditional restrictions related to RD. Moreover, current developments have allowed scholars to train systems depending on extensive database and further tunes these techniques on small database related to RD. Li et al. [16] discussed the occurrence of many RDs in unique regions of China using online research findings.

A dual-phase technique has been designed for forecasting the RD occurrences with users' intentions expressed during the sessions. Initially, an integration of LSTM and Multilayer Perceptron (MLP) technique has been utilized, and then a Linear Regression (LR) algorithm to predict the occurrences of several RDs. The Advanced Neural Networks (ANN) by innovative AI and ML can transform and offer modern solutions for medical management pathways for RD., Multiple RD are more complex to treat and diagnose. Initial support and knowledge is limited, making the disease journey more difficult and lonelier. Higher education systems supporting specific RD are even scarcer, as is support for research on those conditions. The challenges of shifting toward individualized, ways of shifting toward symptom-driven for community and individual-driven medical care solutions are becoming more achievable, increasing the importance of developing under symptom-driven approaches to medical care solutions.

The proposed work integrates synthetic image generation and explainable deep learning to create a unified system for diagnosing and making diagnoses on rare skin diseases in a progression-aware manner. Traditional studies typically apply one or more of the above methods, but not in combination; the proposed method is applied to the generation of realistic synthetic images, feature extraction by channel attention, sequential feature learning, automatic hyperparameter optimization, and explainability visualization of the prediction. This integrated design enhances the accuracy of diagnosis, robustness of the model, transparency and clinical interpretation.

3. Proposed PASLF-RSDD Model

In this section, the design of the proposed PASLF-RSDD rare disease classification system is explained. Figure 1 shows Overall Framework of PASLF-RSDD model.

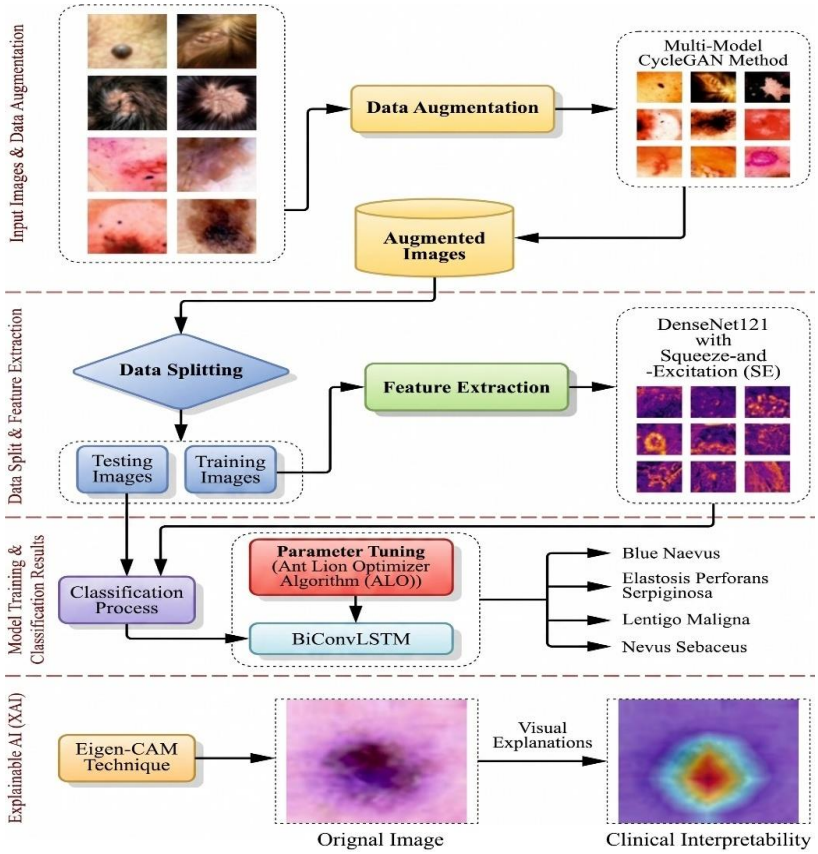

Fig. 1 Overall framework of PASLF-RSDD model

The PASLF-RSDD work consists of five key stages: Synthetic data generation, feature extraction, classification, hyperparameter tuning, and XAI analysis. Initially, the model integrates multi-modal CycleGAN to create realistic and progression-aware synthetic images to alleviate limitations caused by a lack of data in rare disease studies. Then, the feature extraction is performed using DenseNet121 with SE. The SE-augmented DenseNet121 refines channel-wise attention, boosting the representation of fine-grained, often hidden, pathological markers in skin images.

Moreover, the BiConvLSTM model is used to classify the four types of rare skin disease based on the extracted feature representations, and the model parameters of the BiConvLSTM technique are optimized using the ALO algorithm, resulting in improved training stability and model generalization. Finally, the Eigen-CAM is incorporated to offer clear insights into the model's predictions and enhance transparency. These stages are intended to accurately classify rare skin diseases, which makes the system more effective and versatile for real-time use.

3.1. Dataset Details

The DermaEvolve dataset [18] is an extensive collection of skin sores images, collected from publicly accessible datasets and extended with further RD. This dataset intends to support in the improvement and assessment of ML techniques for skin-related diagnosis. To improve variety, the succeeding rare skin disease are exhibited in Table 1.

Table 1. Details of dataset

Skin Rare Diseases	Original Images	Synthetic Images
Elastosis Perforans Serpiginosa	352	1760
Lentigo Maligna	473	2365
Nevus Sebaceus	350	1750
Blue Naevus	482	2410
Total Images	**1657**	**8285**

3.2. Multi-Modal CycleGAN-based Synthetic Data Generation

Deep learning model accuracy in diagnosing rare skin diseases is highly dependent on the amount of training data. Publicly-accessed datasets are commonly small in size and do not typically have a large number of images, making this a class imbalance problem and resulting in poor generalization of the model in the real-world. To overcome this drawback, the proposed PASLF-RSDD framework introduces a Multi-Modal CycleGAN to produce disease-specific visual features preserved progression-aware fake dermoscopic images.

The proposed approach does not just assume the set of prevalent appearances of the lesions, but learns the underlying distribution of lesion appearances, and creates realistic synthetic samples that are close to real clinical observations, not just flips, rotations or scaling of images. The multimodal capability allows multiple plausible visual variations to be generated from a single given image by adding latent style representations, while preserving the pathological identity of the lesion, increasing intra-class diversity without changing the identity of the image's lesion. In Adversarial Learning, the generator continuously learns to generate visually realistic images while the discriminator distinguishes generated images from real dermoscopic images during adversarial training. The cycle-consistency mechanism maintains the structural information by maintaining the important morphological information of the original lesion in the generated image during domain translation. These synthetic images are then combined with the original DermaEvolve dataset to create a balanced dataset of images to be used for further learning stages.

$$I_{syn} = G(I_{org}, z) \quad (1)$$

Where I_{org} denotes original dermoscopic image,$G(.)$ represents the Multi-Modal CycleGAN generator, z is the latent style representation, and I_{syn} is the generated progression-aware synthetic image.

3.3. Deep Feature Extraction with DenseNet121 and SE Blocks

The proposed PASLF-RSDD framework uses DenseNet121 as the backbone feature extractor due to its dense connectivity mechanism, which helps to efficiently propagate information through the network, while promoting feature reuse. This architecture retains the subtle characteristics of the image at the lower level and important semantic information at the higher level that are necessary for the identification of rare skin diseases with a similar morphology. Due to the differences in the size of the lesions, pigmentation, illumination and the extent of the surrounding healthy skin, it is important to extract representative features before classification of dermoscopic images.

The DenseNet121 is improved by the addition of Squeeze-and-Excitation (SE) attention blocks in the dense feature learning process, which enhances the discriminative capability. The SE mechanism learns the channel-wise dependencies from the extracted channel-wise activation maps and automatically determines relationship between individual feature channels. The attention weights are high for informative channels that show clinically relevant lesion characteristics, and suppressed for channels that contain redundant background information.

This adaptive feature recalibration helps the network focus on the boundaries of the lesions, pigmentation patterns, irregularities in texture, and structural variations, which lead to accurate disease identification. The DenseNet121 combined with SE attention produces compact informative deep feature

representations with minimal irrelevant image content while keeping disease-specific information. The resulting feature vectors are then sent to the Bi-directional Convolutional LSTM (BiConvLSTM) classifier, allowing the proposed framework to achieve robust disease classification results in low data volume.

$$F_{SE} = W_{SE} \odot D(I_{syn}) \quad (2)$$

where $D(\cdot)$denotes the DenseNet121 feature extractor, W_{SE} represents the channel attention weights learned by the Squeeze-and-Excitation module, $\odot$ denotes element-wise multiplication, and F_{SE} is the recalibrated deep feature representation.

3.4. Rare Skin Disease Classification Module

The refined deep features obtained from DenseNet121-SE network are fed into the Bidirectional Convolutional Long Short-Term Memory (BiConvLSTM) network to classify the disease. The proposed classifier exploits the correlations between multiple feature representations, while learning them before assigning the final disease category, unlike conventional fully connected classifiers, which simply process extracted features independently. Rare skin diseases often share similar visual traits such as: identical pigmentation, blurry borders of lesions, and complex distributions of skin texture.

Therefore, to make an accurate diagnosis, the classifier must learn to relate several of the discriminative features instead of working with each one separately. The bidirectional learning mechanism allows the network to learn forward and backward at the same time, so complementary contextual information can be fed in while predicting. Embedded in the recurrent architecture, the convolutional operations are able to maintain the spatial structure of the lesion features throughout the learning process and thus enhance the representation of finer pathological patterns that are able to differentiate between visually similar classes of diseases.

The output of both the directional branches is combined for a complete feature representation before the final classification is performed. The classifier then calculates the probabilities of each of the disease categories and classifies the disease that has the highest probability. This classification approach enhances the robustness of the approach to intra-class variability and inter-class similarity, typical difficulties in the diagnosis of rare skin diseases.

$$\hat{Y} = \text{Softmax}(B(F_{SE})) \quad (3)$$

where $B(\cdot)$ denotes the BiConvLSTM classifier, F_{SE} represents the refined deep feature vector, and $\hat{Y}$ denotes the predicted probability distribution over the rare skin disease classes.

3.5. Hyperparameter Optimization using Ant Lion Optimizer

The learning ability of the BiConvLSTM Classifier is directly influenced by such parameters as the learning rate, batch size, dropout probability, number of hidden units and network depth. These parameters are often determined by trial and error and are manually adjusted, which is a labor-intensive process and may not always give the best set of parameters for complex medical image classification problems. In order to overcome this limitation, the proposed PASLF-RSDD framework includes the Ant Lion Optimizer (ALO) as an automatic hyperparameter optimization strategy. Each candidate solution is associated with a different set of hyperparameters of the BiConvLSTM in predetermined ranges during optimization. The candidate configurations are assessed by training the classifier and assessing its validation performance with the classification objective function.

The optimization process continuously improves the search by favoring good solutions and discarding bad parameter combinations, according to the fitness values obtained. This iterative search approach allows the optimizer to strike a balance between the global and local search and thus increase the chance of finding an optimum hyperparameter configuration. The parameter set that is finally obtained by ALO is then used to complete the training of the full model with the synthesized image set at the synthetic image generation stage above. Automatic optimization minimizes the need for manual parameter selection and makes the convergence stable during learning. In terms of classification accuracy, optimized BiConvLSTM classifier demonstrates better performance over various disease classes, faster convergence and better generalization ability.

$$\theta^* = \arg\min_{\theta} L_{val}(\theta) \quad (4)$$

where θ denotes the set of BiConvLSTM hyperparameters, L_{val} represents the validation loss, and θ^* is the optimal hyperparameter configuration identified by the Ant Lion Optimizer.

3.6. Visual Interpretability Analysis using Eigen-CAM

Eigen-CAM is an evolving XAI technique progressively applied to rare disease detection in medical imaging [23]. In contrast to classical Grad-CAM, which relies on class-specific gradients for generating heatmaps, Eigen-CAM recognizes the most dominant patterns in feature representations utilizing Principal Component Analysis (PCA) on convolutional feature maps.

Moreover, instead of using gradient-weighted features, Eigen-CAM derives its maps through computing the principal components of the convolutional layers, eliminating the necessity for backpropagation. Taking the last convolutional layer as input,

- SVD is applied to minimize the integrated activation map A with the input X as represented in mathematical form, $A = U \sum V^t$.
- The CAM offers a well-predicted 1st V matrix eigenvector.
- The estimation emphasizes the principal components regarding the activation map.

From this approach, the ReLU activation function is not used in this one. Theoretically, the Eigen-CAM is determined by,

$$L_{Eigen-CAM} = AV_1 \quad (5)$$

Here, V_1 signifies the 1st eigenvector in the 1st place of the V matrix.

4. Results and Discussion

The proposed PASLF-RSDD framework was validated using the DermaEvolve benchmark dataset of dermoscopic images of four clinically significant rare skin diseases (Elastosis Perforans Serpiginosa, Lentigo Maligna, Nevus Sebaceus, Blue Naevus). The dataset includes 1657 original images, and through the proposed Multi-Modal CycleGAN, the dataset was expanded to 8285 synthetic images, including 9942 images for experimental testing. Images were first normalized, and data augmented before feature extraction, and then resized to 224 × 224 pixels.

To check the generalization ability of the proposed framework, the dataset was first split into 80:20 and then 70:30 training-testing partitions. Table 2 gives a summary of detailed characteristics of the dataset, and Table 3 shows the disease-wise image distribution.

Table 2. Description of the DermaEvolve dataset

Attribute	Description
Dataset Name	DermaEvolve Dataset
Dataset Type	Public benchmark dermoscopic image dataset
Application Domain	Rare skin disease detection and classification
Number of Disease Classes	4 (Elastosis Perforans Serpiginosa, Lentigo Maligna, Nevus Sebaceus, Blue Naevus)
Total Original Images	1,657
Total Synthetic Images	8,285
Total Images Used	9,942
Image Modality	Dermoscopic skin lesion images
Image Format	RGB color images
Image Resolution	Resized to 224 × 224 pixels during preprocessing

Table 3. Disease-wise image distribution

Rare Skin Disease	Original Images	Synthetic Images	Total Images
Elastosis Perforans Serpiginosa	352	1,760	2,112
Lentigo Maligna	473	2,365	2,838
Nevus Sebaceus	350	1,750	2,100
Blue Naevus	482	2,410	2,892
Total	**1,657**	**8,285**	**9,942**

4.1. Experimental Setup

The proposed model, called PASLF-RSDD was implemented with Python 3.11, PyTorch 2.2 (Deep learning framework) software. The proposed model is named PASLF-RSDD, and it is implemented with Python 3.11, PyTorch 2.2 (Deep learning framework) software.

All the experiments were run on a workstation with 1x Intel Core i9-13900K CPU, 64 GB of DDR5 memory, NVIDIA RTX 4090 24 GB GDDR6X with Ubuntu 22.04 LTS OS. The CUDA 12.1 toolkit and cuDNN library were used to speed up the training and inference of the model. The synthetic image generation, deep feature extraction, hyperparameter optimization and explainability analysis were all executed efficiently in the experimental environment.

Before training, all images were resized to 224 x 224 and normalized. Data augmentation techniques used were rotation, flipping, scaling, brightness adjustment and color jittering. Evaluation of the model was done on a data split of 80:20 and 70:30. Adam optimization was used for training BiConvLSTM, while the hyperparameters of ALO were optimized automatically for better convergence and classification accuracy. Table 4 summarizes the optimized hyperparameters obtained through the ALO search process.

Table 4. Optimized hyperparameter values of PASLF-RSDD through ALO

Hyperparameter	Search Range	Optimized Value
Learning Rate	1×10^{-4} - 1×10^{-2}	0.001
Batch Size	16 - 64	32
Number of Epochs	100 - 300	200
Hidden Units (BiConvLSTM)	64 - 512	256
Number of BiConvLSTM Layers	1 - 4	2
Dropout Rate	0.20 - 0.60	0.40
Weight Decay	1×10^{-6} - 1×10^{-3}	1×10^{-5}
Optimizer	Adam, SGD, RMSProp	Adam

Population Size (ALO)	20 - 100	50
Maximum Iterations (ALO)	50 - 200	100
Activation Function	ReLU, Leaky ReLU	ReLU

The classification performance of the proposed PASLF-RSDD framework with 80:20 and 70:30 training-testing partition is shown in Figure 4. The confusion matrices of the training and testing set of the four corresponding rare skin diseases are shown in Figures 2(a)-(d), and it is observed that most samples are correctly classified into their respective classes of rare skin diseases. The high value concentration along the main diagonal implies high accuracy of the classification with a small amount of misclassification between class, indicating that the proposed framework is good at differentiating visually similar skin lesions. The learned feature representations are shown to be robust, as only a few of the samples are misclassified.

The Precision-Recall (PR) curves of the two experimental settings are shown in Figures 2(e) and (g). All the curves are still in the upper-right section, suggesting high precision and recall for all the disease categories, even under class imbalance. The Receiver Operating Characteristic (ROC) curves, as shown in Figures 2(f) and (h), have a large area under the curve, and all curves are approaching the upper left corner. Such results show a good discriminative power and a robust classification capability regardless of the training-testing split as done. The same behavior seen in each confusion matrix, PR curve and ROC curve demonstrates reliable and generalised rare skin disease classification using the proposed PASLF-RSDD framework.

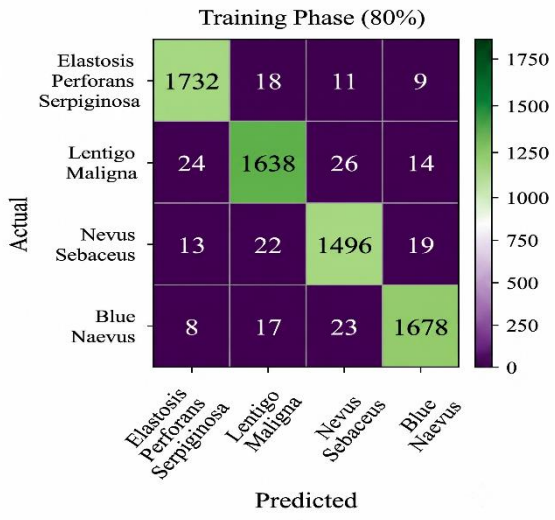

(a)

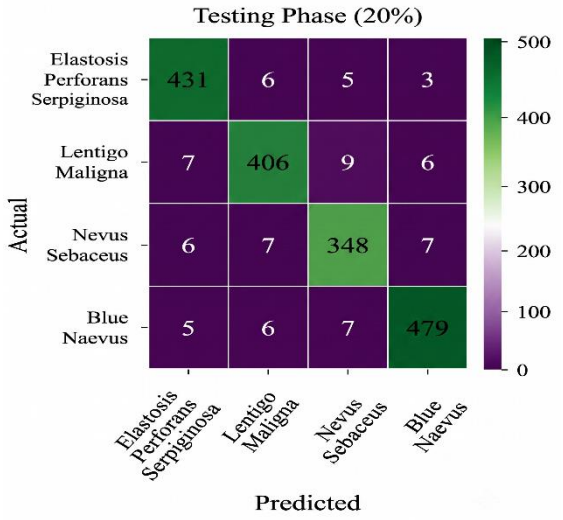

(b)

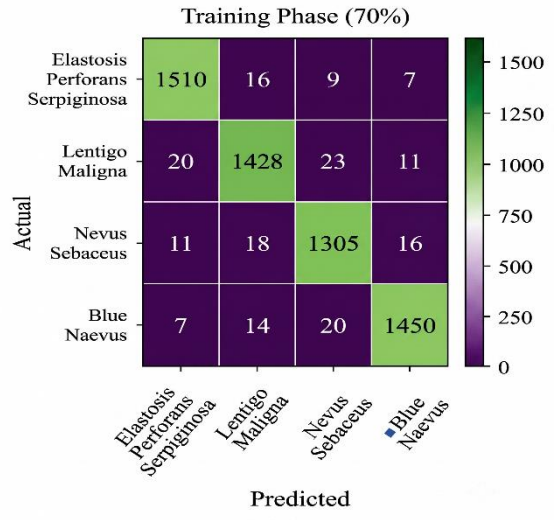

(c)

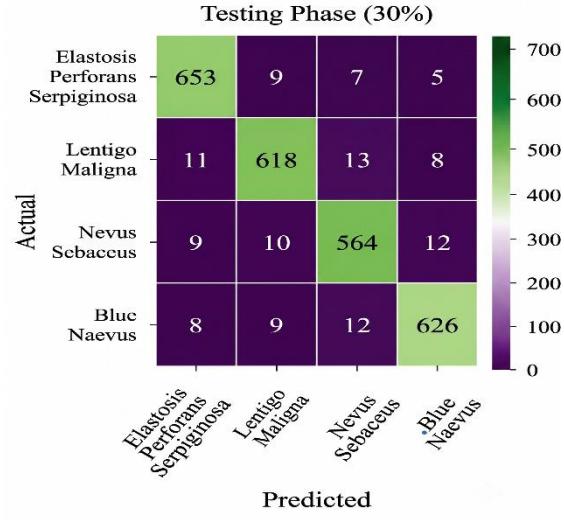

(d)

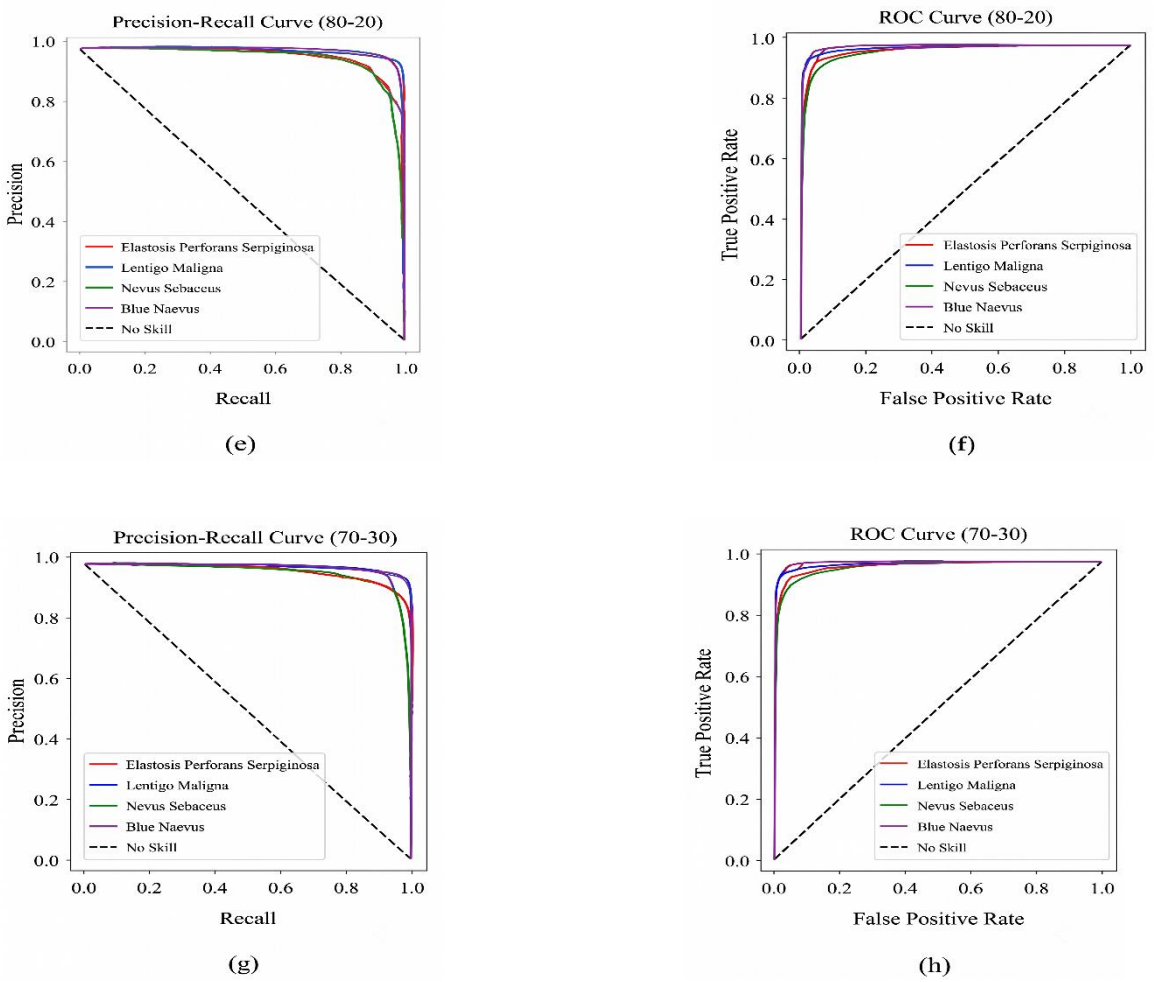

Fig. 2 Classifier result of PASLF-RSDD method with (a)-(d), Confusion matrices, and (e)-(h) PR/ROC curves under 80:20 and 70:30.

Table 5 shows the RD classifier outcomes of the PASLF-RSDD model with 80:20.

The outcomes imply that the PASLF-RSDD approach precisely identified the samples. On 80% TRAP, the PASLF-RSDD technique gives average value with an accuracy of 97.31%, a precision of 94.21%, a sensitivity of 94.42%, specificity of 98.24%, and F_{score} of 94.30%, respectively. Meanwhile, on 20% TESP, the PASLF-RSDD model offers average value with accuracy of 97.37%, precision of 94.50%, a sensitivity of 94.58%, specificity of 98.27%, and F_{score} of 94.53%, respectively.

Table 5. Rare diseases classifier result of PASLF-RSDD method with 80:20

Class Labels	Accuracy	Precision	Sensitivity	Specify	F_{score}
TRAP (80%)					
Elastosis Perforans Serpiginosa	96.58	91.96	91.76	97.86	91.86
Lentigo Maligna	97.89	96.84	95.82	98.73	96.33
Nevus Sebaceus	96.82	90.69	94.43	97.45	92.52
Blue Naevus	97.98	97.37	95.66	98.93	96.50
Average	**97.31**	**94.21**	**94.42**	**98.24**	**94.30**
TESP (20%)					
Elastosis Perforans Serpiginosa	96.80	92.84	92.58	97.99	92.71
Lentigo Maligna	97.71	95.97	95.55	98.51	95.76
Nevus Sebaceus	96.68	91.51	93.75	97.52	92.62
Blue Naevus	98.31	97.66	96.43	99.07	97.04
Average	**97.37**	**94.50**	**94.58**	**98.27**	**94.53**

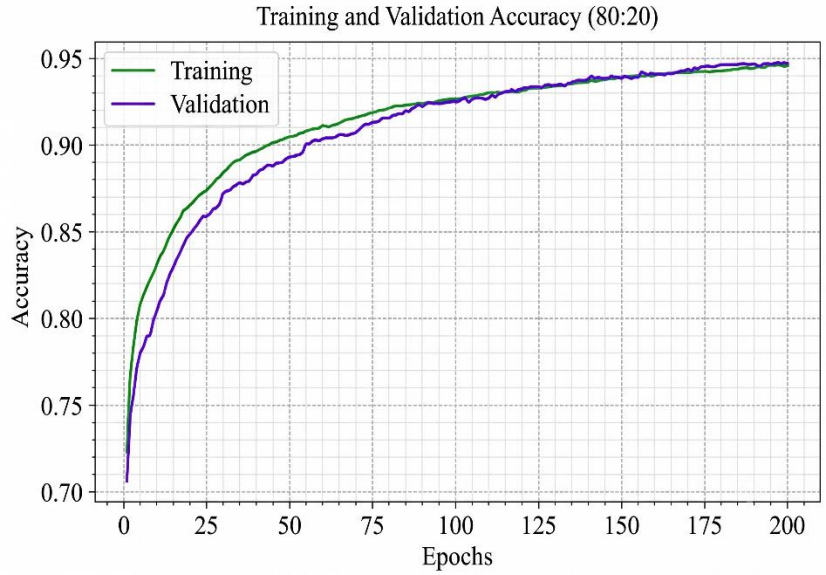

Fig. 3 Accu*racy* curve of PASLF-RSDD method with 80:20

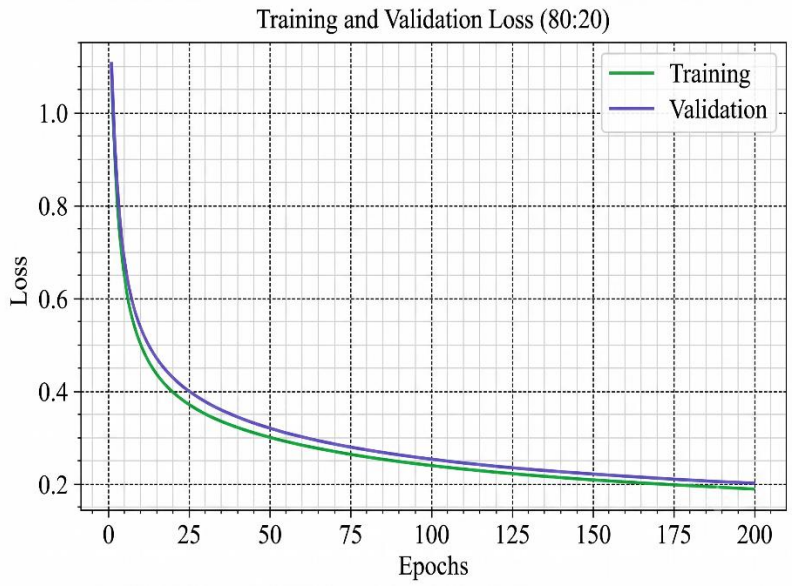

Fig. 4 Loss curve of PASLF-RSDD approach with 80:20

Figure 4 represents the TRAIN and VALID loss curves of the PASLF-RSDD technique with an 80:20 training-testing split over 200 epochs. Both losses reduce closely when the early epochs, signifying quick learning, and then progressively deny in a stable and smooth manner, representing efficient integration. The consistent overlap among training and validation loss, with only a small and constant gap, implies lesser over-fitting and robust generality.

Table 6 shows the RD classifier outcomes of the PASLF-RSDD model at 70:30. The outcomes imply that the PASLF-RSDD system precisely classified the samples. On 70% TRAP, the PASLF-RSDD approach achieves average value with accuracy of 98.49%, precision of 97.03%, sensitivity of 96.93%, specificity of 98.98%, and F_{score} of 96.97%, respectively. Meanwhile, on 30% TESP, the PASLF-RSDD model delivers average value with accuracy of 98.43%, precision of 97.06%, sensitivity of 96.85%, specificity of 98.92%, and F_{score} of 96.95%, respectively.

Figure 5 display the TRAIN and VALID accuracy curves of the PASLF-RSDD model on 70:30 training-testing split across 200 epochs. TRAIN accuracy increases constantly and attains a higher level, signifying efficient learning and integration. The VALID accuracy sharply succeeds the training trend with a stable and small gap, validating good generalization and least overfitting.

Table 6. Rare diseases classifier result of PASLF-RSDD method with 70:30

Class Labels	Accuracy	Precision	Sensitivity	Specificity	F_{score}
TRAP (70%)					
Elastosis Perforans Serpiginosa	98.48	96.60	96.28	99.08	96.44
Lentigo Maligna	98.28	96.97	96.97	98.80	96.97
Nevus Sebaceus	98.91	97.91	96.86	99.46	97.38
Blue Naevus	98.29	96.63	97.59	98.58	97.11
Average	**98.49**	**97.03**	**96.93**	**98.98**	**96.97**
TESP (30%)					
Elastosis Perforans Serpiginosa	98.87	98.24	96.36	99.54	97.29
Lentigo Maligna	97.87	96.63	95.96	98.64	96.29
Nevus Sebaceus	99.03	98.31	97.22	99.54	97.77
Blue Naevus	97.95	95.05	97.88	97.98	96.45
Average	**98.43**	**97.06**	**96.85**	**98.92**	**96.95**

Figure 6 demonstrates the TRAIN and VALID loss curves of the PASLF-RSDD method with a 70:30 training-testing split over 200 epochs. Both losses reduce closely when the early epochs, signifying quick learning, and then progressively deny in a stable and smooth manner, representing efficient integration. The consistent overlap among training and validation loss, with only a small and stable gap, imply least over-fitting and robust generality.

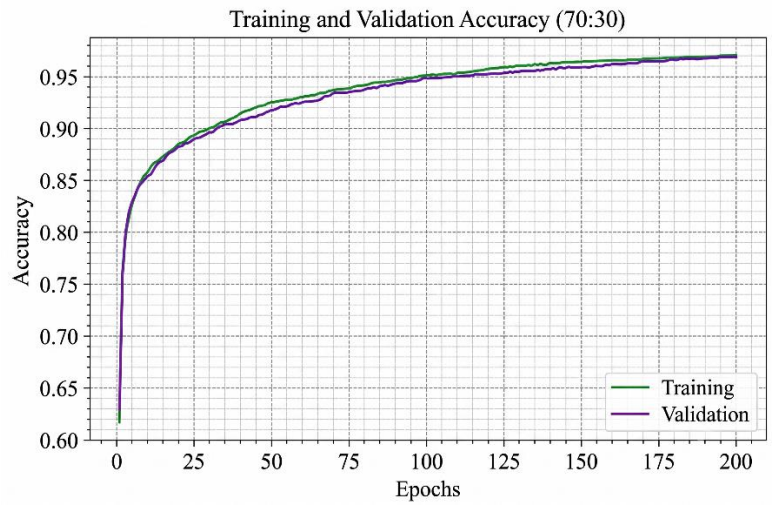

Fig. 5 Accuracy curve of PASLF-RSDD method with 70:30

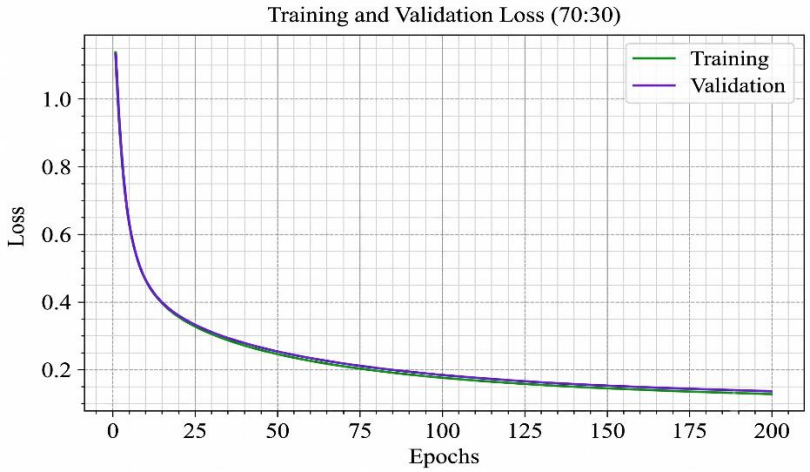

Fig. 6 Loss curve of PASLF-RSDD approach with 70:30

The comparative results of PASLF-RSDD techniques with present methods with different measures and error rate are validated in Table 7 [24, 25]. The simulation results specified that the PASLF-RSDD model outperformed improved performances.

According to varied metrics, the PASLF-RSDD approach have attained better performance with accuracy of 98.49%, precision of 97.03%, sensitivity of 96.93%, and F_{score} of 96.97%, where the ANN, XGBoost, Gboost, Decision Tree (DT), TabNet, LIghtGBM and CatBoost algorithms have slightly low performance, respectively. In the meantime, depend on error rate, the PASLF-RSDD method have attained low performance with error rate of 1.51% when the ANN, XGBoost, Gboost, DT, TabNet, LIghtGBM and CatBoost method have achieves better outcomes with error rate of 6.00%, 16.00%, 15.60%, 21.10%, 32.60%, 22.90% and 20.90%, respectively.

Table 7. Comparative result of PASLF-RSDD method with existing approaches

Methods	Accuracy	Error Rate (%)	Precision	Sensitivity	F_{score}
ANN	94.00	6.00	90.06	90.59	83.19
XGBoost	84.00	16.00	90.93	87.31	82.73
Gboost	84.40	15.60	82.26	83.53	93.97
Decision Tree	78.90	21.10	93.55	93.65	92.64
TabNet	67.40	32.60	86.42	88.20	95.02
LIghtGBM	77.10	22.90	73.98	89.24	82.96
CatBoost	79.10	20.90	90.44	93.05	79.43
PASLF-RSDD	**98.49**	**1.51**	**97.03**	**96.93**	**96.97**

The Eigen-CAM visualisations for some representative images of rare skin diseases are presented in Figure 7. The activation maps presented clearly illustrate the consistent focus on clinically relevant lesion regions, as opposed to surrounding background information, in the proposed PASLF-RSDD approach. The activation responses are mostly observed around the borders of the lesions, around the pigmentation patterns and around variations in texture; this is a sign that the classifier is able to capture discriminative pathological characteristics which are associated with each disease category.

The results of the visualization show that each disease class has a different distribution of activations depending upon their morphological features. The Lentigo Maligna and Blue Naevus show more activation in the pigmented areas, while Elastosis Perforans Serpiginosa shows more activation within the characteristic lesion structures. Nevus Sebaceus shows local reactions reflecting the pattern of sebaceous lesions. The above observations show that the framework learns disease-specific visual representation as opposed to using irrelevant image regions.

The model is consistent across disease categories, suggesting that predictions are based on meaningful image features of the disease. This visual evidence has the advantage of making the diagnostic process more interpretable and thus giving more confidence that the classifier is focused on clinically relevant characteristics of the lesions. The improved explanation strengthens the argument for the potential of the proposed PASLF-RSDD system as an interpretable decision-support system for the diagnosis of rare skin diseases, improving the possibility of its clinical use.

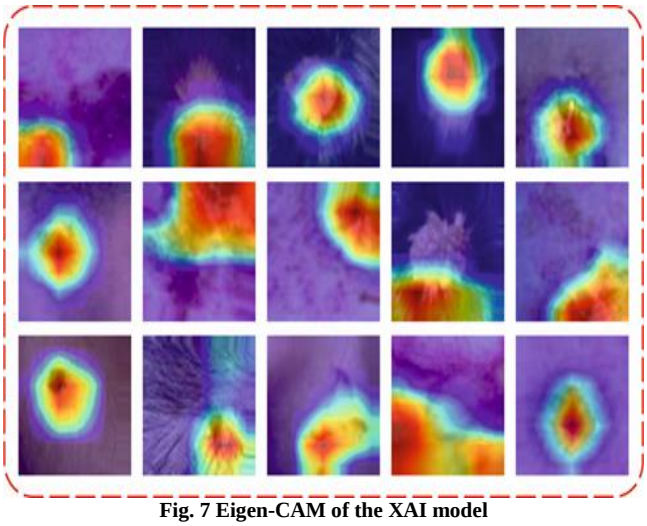

Fig. 7 Eigen-CAM of the XAI model

5. Conclusion

In this article, the PASLF-RSDD approach has been presented for improving rare skin disease diagnosis via multi-modal synthetic data augmentation, thus enhancing the performance of the DL system. Primarily, the proposed PASLF-RSDD technique utilized Multi-Modal CycleGAN for synthetic image generation. Subsequently, high-level discriminative features are captured with DenseNet121 with SE blocks for better feature representation. The captured features are fed into a BiConvLSTM architecture for precise rare skin condition classification. Additionally, the ALO algorithm is leveraged for fine-tuning the hyperparameters of the classifier, heightening convergence stability and model performance. Lastly, by integrating the Eigen-CAM method in the proposed model, the model's predictions become more interpretable and clinically meaningful, supporting automated

rare skin disease classification systems. The experimental results of the PASLF-RSDD model are conducted on the benchmark DermaEvolve Dataset, and the comparative results prove the supremacy of the PASLF-RSDD model in rare disease classification, such as Elastosis Perforans Serpiginosa, Lentigo Maligna, Nevus Sebaceus, and Blue Naevus, achieving an accuracy of 98.49 % and error rate of 1.51% compared to existing models across diverse performance measures.

Conflicts of Interest

The authors declare that there is no conflict of interest regarding the publication of this paper.

Funding Statement

The authors declare that no specific funding was received from any agency for conducting this research work.

References

[1] Mengqiao He et al., "FPGDKG 1.0: An Integrated Facial Phenotype-Gene-Disease Knowledge Graph for Rare Disease Diagnosis and Explanation," *IEEE Journal of Biomedical and Health Informatics*, pp. 1-10, 2026. [CrossRef] [Google Scholar] [Publisher Link]

[2] Shahnazeer Chembalakkat Kunjumohamad, and Sureshkumar Govindaraj, "NLP-Driven Federated Learning Framework for Multi-Organ Rare Disease Prediction," *Iran Journal of Computer Science*, vol. 9, no. 1, 2026. [CrossRef] [Google Scholar] [Publisher Link]

[3] Kimberly F.Greco et al., "A Weakly Supervised Transformer for Rare Disease Diagnosis and Sub Phenotyping from EHRs with Pulmonary Case Studies," *npj Digital Medicine*, vol. 9, no. 1, pp. 1-13, 2026. [CrossRef] [Google Scholar] [Publisher Link]

[4] Richard Noll et al., "Enhancing Diagnostic Precision for Rare Diseases using Case-based Reasoning," *Journal of the American Medical Informatics Association*, vol. 33, no. 1, pp. 98-111, 2026. [CrossRef] [Google Scholar] [Publisher Link]

[5] Ana M.B. Amorim et al., "Artificial Intelligence in Rare Diseases: Toward Clinical Impact," *Trends in Pharmacological Sciences*, vol. 46, no. 12, pp. 1241-1268, 2025. [CrossRef] [Google Scholar] [Publisher Link]

[6] Serena Lembo et al., "AI4RDD: Artificial Intelligence and Rare Disease Diagnosis: A Proposal to Improve the Anamnesis Process," *Image and Vision Computing*, vol. 162, 2025. [CrossRef] [Google Scholar] [Publisher Link]

[7] M. Mendez et al., "Leveraging Domain Knowledge for Synthetic Ultrasound Image Generation: A Novel Approach to Rare Disease AI Detection," *International Journal of Computer Assisted Radiology and Surgery*, vol. 20, no. 2, pp. 415-431, 2024. [CrossRef] [Google Scholar] [Publisher Link]

[8] Lucas Cortial et al., "Artificial Intelligence in Drug Repurposing for Rare Diseases: A Mini-Review," *Frontiers in Medicine*, vol. 11, pp. 1-7, 2024. [CrossRef] [Google Scholar] [Publisher Link]

[9] Shanavaz Mohammed et al., "A Review of AI-Powered Diagnosis of Rare Diseases," *International Journal of Current Science Research and Review*, vol. 7, no. 9, pp. 6837-6843, 2024. [CrossRef] [Google Scholar] [Publisher Link]

[10] Felix Haller et al., "Utilizing Artificial Intelligence and Next-Generation Sequencing to Facilitate the Diagnosis of Rare Diseases," *Clinical Kidney Journal*, vol. 17, no. 1, pp. 1-2, 2024. [CrossRef] [Google Scholar] [Publisher Link]

[11] Xi Chen et al., "RareAlert: Aligning Heterogeneous Large Language Model Reasoning for Early Rare Disease Risk Screening," *arXiv preprint*, pp. 1-28, 2026. [CrossRef] [Google Scholar] [Publisher Link]

[12] Jingyu Tang, "Multi-Modal Fusion and Transferable Deep Learning for Rare Disease Detection: A CNN-Transformer Framework with Cross-Domain Adaptation on Limited CT and MRI Data," *Advances in Engineering Innovation*, vol. 16, no. 6, pp. 144-148, 2025. [CrossRef] [Publisher Link]

[13] Xin Wang, Da He, and Chunlin Jin, "AI-Driven Enhancements in Rare Disease Diagnosis and Support System Optimization," *Intractable and Rare Diseases Research*, vol. 14, no. 4, pp. 306-308, 2025. [CrossRef] [Google Scholar] [Publisher Link]

[14] Giulio Napolitano et al., "Potential of Artificial Intelligence to Accelerate Drug Development for Rare Diseases," *Pharmaceutical Medicine*, vol. 38, no. 2, pp. 79-86, 2024. [CrossRef] [Google Scholar] [Publisher Link]

[15] Magda Wojtara et al., "Artificial Intelligence in Rare Disease Diagnosis and Treatment," *Clinical and Translational Science*, vol. 16 no. 11, pp. 2106-2111, 2023. [CrossRef] [Google Scholar] [Publisher Link]

[16] Jiayu Li et al., "Estimating Rare Disease Incidences with Large-Scale Internet Search data: Development and Evaluation of a Two-Step Machine Learning Method," *JMIR Infodemiology*, vol. 3, no. 1, pp. 1-13, 2023. [CrossRef] [Google Scholar] [Publisher Link]

[17] Chaitran Chakilam, and Aaluri Seenu, "Transformative Applications of AI and ML in Personalized Treatment Pathways: Enhancing Rare Disease Support Through Advanced Neural Networks," *Frontiers in Health Informatics*, vol. 13, no. 8, 2024. [Google Scholar]

[18] Kaggle, DermaEvolve - Augmented unprocessed 64, Kaggle, 2025. [Online]. Available: https://www.kaggle.com/datasets/lokeshbhaskarnr/dermaevolve-augmented-unprocessed-64/data

[19] Ye Eun Kim et al., "Optical Coherence Tomography Image Enhancement and Layer Detection using Cycle-GAN," *Diagnostics*, vol. 15, no. 3, pp. 1-11, 2025. [CrossRef] [Google Scholar] [Publisher Link]

[20] Gunjan Shandilya et al., "Proposed Dense Variational Autoencoder Model Integrated with Contrastive Learning for Foot Ulcer Classification," *Scientific Reports*, vol. 16, no. 1, pp. 1-42, 2026. [CrossRef] [Google Scholar] [Publisher Link]

[21] Yunpeng Chang, and Bin Luo, "Bidirectional Convolutional LSTM Neural Network for Remote Sensing Image Super-Resolution," *Remote Sensing*, vol. 11, no. 20, pp. 1-18, 2019. [CrossRef] [Google Scholar] [Publisher Link]

[22] Amirhosein Hojati et al., "Chaotic Hybrid Meta-Heuristic Optimization Algorithm for Construction Site Layout Planning Problem," *Letters in High Energy Physics*, vol. 2024, pp. 4788-4791, 2024. [CrossRef] [Google Scholar] [Publisher Link]

[23] Mara Giavina-Bianchi et al., "Explainability Agreement Between Dermatologists and Five Visual Explanations Techniques in Deep Neural Networks for Melanoma AI Classification," *Frontiers in Medicine*, vol. 10, pp. 1-13, 2023. [CrossRef] [Google Scholar] [Publisher Link]

[24] Anna Visibelli et al., "The Impact of Artificial Intelligence in the Odyssey of Rare Diseases," *Biomedicines*, vol. 11 no. 3, pp. 1-23, 2023. [CrossRef] [Google Scholar] [Publisher Link]

[25] Irfan Al-Hussaini et al., "An Interpretable Machine Learning Framework for Rare Disease: A Case Study to Stratify Infection Risk in Pediatric Leukemia," *Journal of Clinical Medicine*, vol. 13, no. 6, pp. 1-24, 2024. [CrossRef] [Google Scholar] [Publisher Link]